

The work described in this document was performed by Transportation Technology Center, Inc., a wholly owned subsidiary of the Association of American Railroads.

# Analysis of Conventional and Tapered Bonded Insulated Rail Joints

by David D. Davis (TTCI), Adric Eckstein, Seth Lambrecht and David A. Dillard (Virginia Tech)

## Summary

Under sponsorship of the Association of American Railroads, Transportation Technology Center, Inc. is leading an industry-wide effort to improve the performance of bonded insulated joints (IJs) in heavy axle load (HAL) freight service. This *Technology Digest* describes results of stress analyses done on the current design IJ and a proposed improved design. Analyses conducted by numerical and classical methods show:

- The two methods are in agreement with each other on stresses and deflections. They also corroborate the predominant failure mode, epoxy cracking, seen in the field.
  - The conventional butt-jointed IJ (CJ) is less vertically stiff than the rail. A CJ will deflect 10 percent more than the parent rail in good track.
  - Predicted maximum epoxy shear stresses for a CJ in HAL service are above 6000 psi. This is well above the recommended service loads for the epoxies currently used.
- A tapered joint design (TJ), with overlapping “angle cut” rail ends, will have significant advantages over the CJ design used today. These include:
  - Reduced deflections (20% less than CJ and 10% less than rail).
  - Significantly lower maximum epoxy shear stresses – about 1/3 of the CJ design. This will lower maximum stresses below epoxy recommended service loads.
  - An additional glued surface (between the rail ends). This will provide increased longitudinal strength.
- The width of the end-post gap between the two rails has little effect on CJ deflections and epoxy stresses, for a given load. However, a wider end post may increase the dynamic loads caused by a wheel crossing a larger end-post gap.
- Effects of longitudinal rail forces:
  - Generally, longitudinal static loads are less significant than live loads.
  - Tensile forces will change location of maximum epoxy stress from top to bottom of joint bar (near the end post).
- Effect of Fasteners:
  - Due to the bolt-hole insulation and relative stiffness of the IJ, the fasteners only provide clamping force for the joint. They should not carry any vertical load until the epoxy fails.

Virginia Polytechnic Institute and State University (VA Tech), an AAR affiliated laboratory, conducted the analysis of conventional and tapered insulated joints described in this report.



**BACKGROUND AND INTRODUCTION**

Insulated rail joints have been used almost exclusively in railroads to provide electrical discontinuity where needed for railroad signal systems. The basic insulated joint configuration, a butt joint with an insulator, remained virtually unchanged for over 100 years. As car capacity increased, the use of epoxy bonding to strengthen the joint has been preferred over other means. With further increased loading on freight lines, bonded rail joints are encountering early breakdown through either electrical or mechanical failure. These freight lines show significant reduction in the lifetime of insulated joints to about 12 to 18 months, significantly lower than other railway components.<sup>1</sup> Train delay costs have significantly increased the desire for an improved joint.

In order to better understand the causes of failure within bonded rail joints, analytical, numerical, and experimental studies have been initiated on representative joints and materials. This *Technology Digest* discusses using the finite element method to develop a numerical analysis of the stresses within the joint’s adhesive layer. It also presents the static stress analysis of the adhesive layer for a conventional bonded rail joint (CJ), as well as a proposed tapered (or angle cut) bonded rail joint (TJ). The numerical solutions developed within this study indicate that the design of a tapered joint to replace the CJ will reduce shear stresses within the adhesive layer and should extend the life of the rail joint.

Commercially available bonded rail joints are typical butt joints consisting of the rails, joint bars, and an epoxy adhesive that often contains a fiberglass cloth layer. Figure 1 shows a cross-section illustration of the joint, taken through one of several bolts used to augment the adhesive. Bond failure can be caused by a combination of factors including mechanical fatigue, environmental degradation of the bond, foundation degradation, and dynamic loading resulting from changes in the rail surface, stiffness, and foundation.

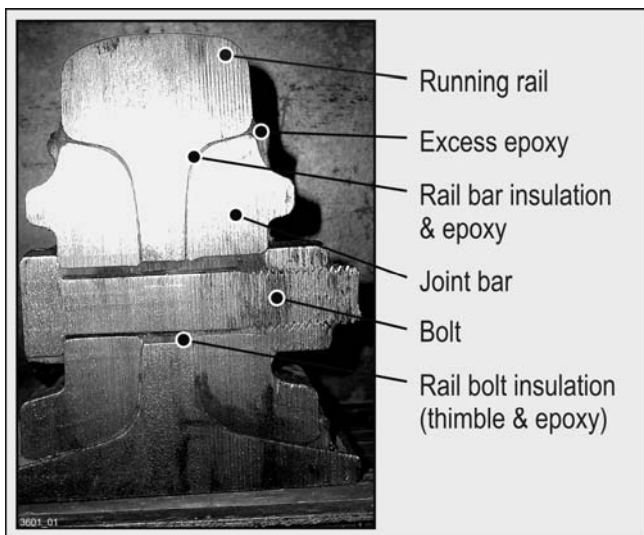


**Figure 1. Cross-Section of a Typical Bonded Insulated Rail Joint<sup>1</sup>**

This study focused on mechanical failure of the adhesive layer by examining static stresses in the epoxy. Although a numerical analysis of the adhesive layer within the CJ has not been conducted, several other failure modes of the joint have been studied previously.

The first reported analytical examination of IJs used beam-on-elastic-foundation models to create a CJ model to describe rail deflections and moments. This joint was a simple, one-dimensional model that used a uniform elastic foundation and experimentally determined stiffness to characterize the behavior of the joint.<sup>2</sup> The current study expands upon the one described in reference 2 and creates analytical solutions for the CJ and the TJ for comparison with numerical models.

**Finite Element Modeling Technique**

The CJ modeled in this study consists of a butt joint of two rails, separated by a 1/4-inch-thick insulating layer known as the end post. Two joint bars on each side of the rails hold the joint together through the use of an adhesive layer and 4 to 6 bolts, depending upon the joint design. The adhesive layer is comprised of epoxy and a fiberglass cloth. A finite element model was constructed for the CJ consisting of two rail sections, two joint bars, and an adhesive layer. Half-plane symmetry was used to simplify the model. Figure 2 shows the finite element model of the CJ. Tie constraints were used to connect adhesive layer nodes to the rail surface nodes. In this preliminary model, only one element through the 1/8-inch-thick adhesive layer was used.

The TJ was created using the same sections as the CJ. However, the TJ used rails tapered at 6.41 degrees, creating a tapered rail length of 10 inches. The finite element model of the TJ is shown in Figure 3. Since the joint can only be tapered across the web section of the rail, a thick web rail, used primarily in bridge sections, was employed to increase the angle of the taper. The web thickness of the rail changed from 11/16 inch to 1 5/8 inches. For this joint, there are no symmetry planes.

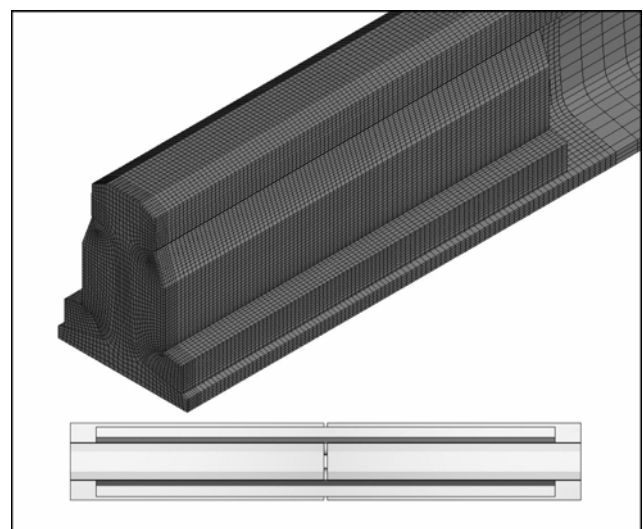


**Figure 2. Finite Element Model of the CJ**

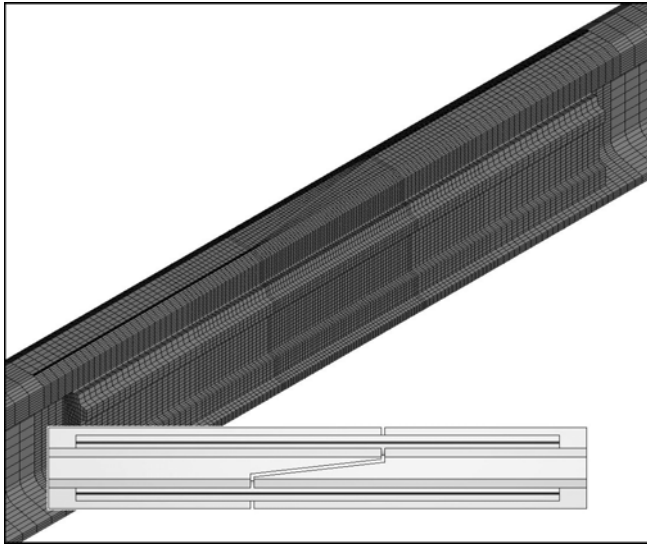


Figure 3. Finite Element Model of the TJ

For the finite element models for the CJ and the TJ, an elastic foundation was used based on a track stiffness of 3000 psi (see Figure 4)<sup>3</sup>. Elastic foundation elements tie surface nodes to spring elements equivalent to a surface stiffness given in  $\text{lb}/\text{in}^3$ . Using the rail base width of 6 inches, the equivalent elastic foundation stiffness at the base of the rail was 500  $\text{lb}/\text{in}^3$ . However, the uniform elastic foundation is the average stiffness and does not account for rail ties. Discrete ties centered under the gap provide a varying elastic foundation, and therefore an equivalent foundation must be used over sections of rail-tie contact. The rail-tie contacts were spaced as a suspended joint commonly used in the railroad industry.<sup>3</sup> Using a unit cell around a tie (10-inch tie width on 30-inch spacing), an elastic foundation of 1500  $\text{lb}/\text{in}^3$  was implemented over the tie contact area.

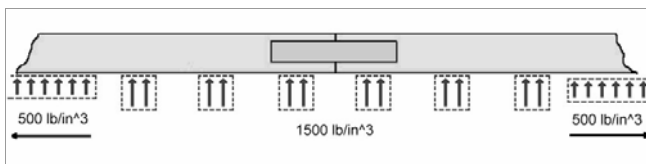


Figure 4. Elastic Foundation Model

Since several designs were examined in this study, the change in boundary conditions at the rail ends was minimized by extending the rail sections 230 inches from the center of the joint, using symmetry conditions at the ends. The rail displacements and moments in the numerical models were compared to analytical solutions to ensure the validity of these boundary conditions.

Three loading conditions were present in each of the rail models: (1) bolt preloads, (2) wheel load, and (3) axial rail tension. Using nonlinear finite element techniques to solve the contact conditions in the bolts can be very intensive.

However, nonlinear solution techniques are not necessary to model these rail joints. The preload in the bolts compresses the rail bars, strengthening the joint. Additionally, each bolt is placed within an insulating thimble that allows for significant slip of the bolt within the sleeve. The shear strain within the adhesive is so small that the deflection of the joint will not overcome the gaps within the bolts and thimbles. As a result, the bolts only have the effect of compressing the joint bars, and were modeled using a 50-kip load applied over the area of each bolt. No holes were included in the models, due to the focus on the adhesive stresses, which are largest well away from the bolts.

The weight of the train was modeled as a static load of evenly distributed pressure over a square inch of rail. Because this analysis focused on stress within the adhesive layer, which is several inches from the surface contact, using this loading condition greatly simplified the model. These models used a wheel load of 32,500 pounds, somewhat lower than the wheel loads on heavy freight lines. However, the 32,500-pound wheel load was used as a common reference load to relate these numerical results to other solutions. The third loading condition is the axial tension that results from cold weather, a design and maintenance feature that prevents the rail from buckling on hot days. Since the average axial load will vary with temperature, two cases of axial tension were examined; i.e., 0 ksi and 200 ksi. The equivalent loads were applied to the rail ends.

## RESULTS AND DISCUSSION

The shear stresses within the adhesive layer were found to be large for an epoxy adhesive. Figure 5 shows the in-plane shear stresses for the CJ. The shear stresses for the bond are shown with the adhesive unwrapped into a flat plane. The cases with and without axial loading are shown in the top and bottom, respectively. Depending upon the axial loading conditions, the in-plane shear stress varies from 5400 to 6400 psi. These stresses should be viewed as estimates due to the crude mesh used within the adhesive layer. Nonetheless, the magnitude does suggest stresses that are larger than common adhesives could withstand under fatigue and environmental exposure conditions.

Differences in axial loading change the location of the critical section within the adhesive. Assuming the shear is positive toward the center of the joint, the top section of the bond has a positive shear, and the bottom section has a negative shear. Axial loading superimposes negative shear along the entire bond height. This loading reduces the shear in the top section and amplifies the shear in the bottom section.

The numerical solutions of the TJ indicate significantly reduced shear stresses. Figure 6 shows the in-plane shear stress for the TJ. The maximum in-plane shear is reduced to a magnitude of 1600 to 1700 psi. The TJ also consists of an adhesive layer along the length of the taper cut. This section shows shear stresses of the same values as the adhesive along the length of the joint bars.

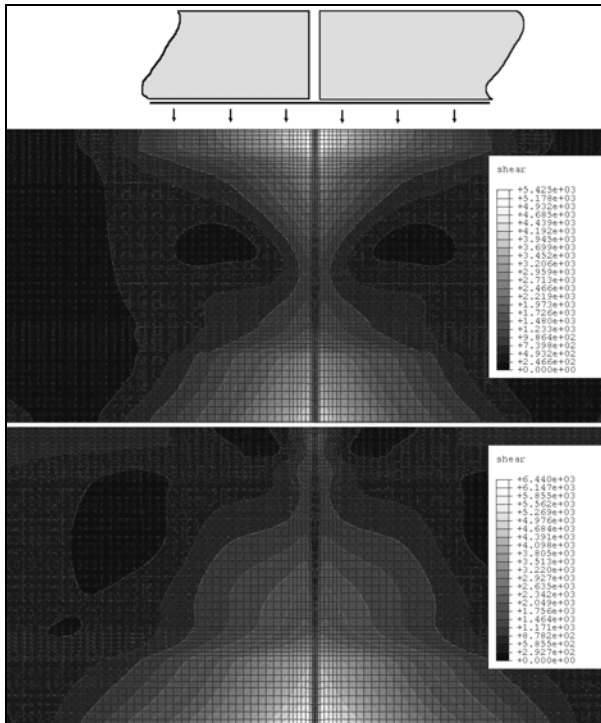


Figure 5. Shear Stresses in the CJ Adhesive Layer. Axial Loads of 0 ksi (Top) and 200 ksi (Bottom)

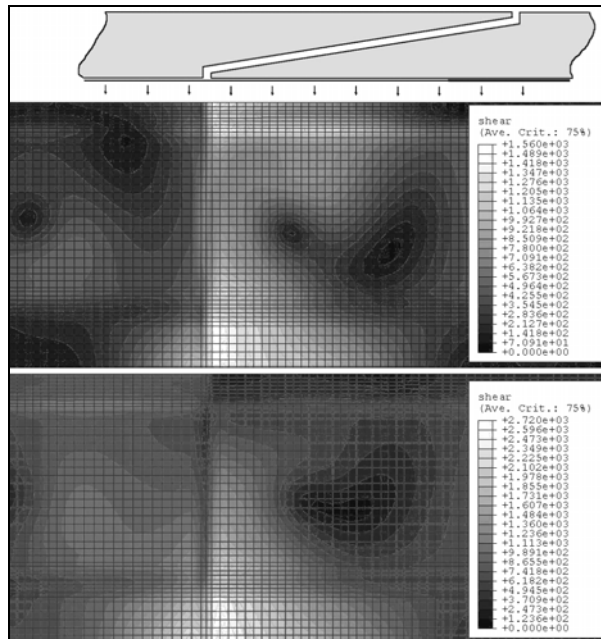


Figure 6. Shear Stresses in the TJ Adhesive Layer. Axial Loads of 0 ksi (Top) and 200 ksi (Bottom)

Figure 7 shows a comparison of predicted epoxy stresses for the CJ and TJ designs. Note that the supplier recommended maximum stress levels for the currently used epoxies are well below the predicted CJ levels. Conversely, the TJ design is predicted to have epoxy stress levels below the supplier recommended maximums. This suggests that railroads will be able to successfully use the existing epoxies in TJ designs, but

should be searching for a much stronger epoxy for use in CJ designs.

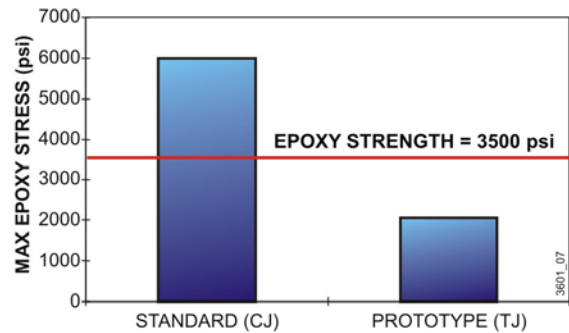


Figure 7. The Effect of IJ Design on Epoxy Stresses

## CONCLUSIONS

Numerical results indicate the presence of high shear stress within the adhesive layer of the CJ. These high shear stresses may result in the degradation of the epoxy within the joint, especially under fatigue and environmental exposure conditions. Changes in axial tension will affect both the magnitude and location of the maximum in-plane shear stress along the bond. The TJ significantly reduces the shear stresses to about a third of the shear stresses present within the CJ. These reductions in shear stress could allow for a longer joint lifetime than the current insulated joint.

## Future Work

Planned work for 2006 will follow up on the findings of the 2005 studies presented in this TD. Prototypes have been developed using the TJ design analysis. Further refinements of the design will be developed upon analysis of field test results. Additionally, work to lower the epoxy stresses and improve the epoxy strength in CJ designs will be conducted. This plan includes epoxy materials, surface preparation, and epoxy reinforcement investigation.

## Acknowledgments

The Association of American Railroads was very supportive of this project. We also acknowledge the interactions with Virginia Tech's Rail Technology Laboratory, directed by Mehdi Ahmadian. We are grateful to these individuals and to Muhammad Akhtar for helpful discussions. We especially acknowledge Heike Lohse-Busch (Research Assistant, Virginia Tech), Prof. Raymond H. Plaut (Department of Engineering Science & Mechanics, Virginia Tech), and Muhammad Akhtar (TTCI) for their work on this project.

## References

1. Davis, D., D. Collard, and D. Guillen, January 2005. "Bonded Insulated Joint Performance in Mainline Track," *Railway Track and Structures*.
2. Kerr, A. D. and J. E. Cox, 1999. "Analysis and tests of bonded insulated joints subjected to vertical wheel loads," *Int. Journal Mechanical Science*, 41, 1253-1272.
3. Kerr, A. D., 2003. *Fundamentals of Railway Track Engineering*, Simmons-Boardman.

Visit our website at <http://www.ttc1.aar.com>